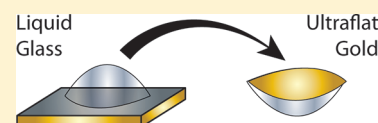


## Solvent-Resistant Ultraflat Gold Using Liquid Glass

James T. Hugall,<sup>\*,†</sup> Alexander S. Finnmøre,<sup>†</sup> Jeremy J. Baumberg, Ulrich Steiner, and Sumeet Mahajan<sup>\*</sup>

Cavendish Laboratory, University of Cambridge, J.J. Thomson Avenue, Cambridge CB3 0HE, U.K.

**ABSTRACT:** Templating against atomically flat materials allows creation of smooth metallic surfaces. The process of adding the backing (superstrate) to the deposited metals has proven to be the most difficult part in producing reliable, large-area, solvent-resistant substrates and has been the subject of recent research. In this paper we describe a simple and inexpensive liquid glass template-stripping (lgTS) method for the fabrication of large area ultraflat gold surfaces. Using our lgTS method, ultraflat gold surfaces with normals aligned along the  $\langle 111 \rangle$  crystal plane and with a root-mean-square roughness of 0.275 nm (over  $1 \mu\text{m}^2$ ) were created. The surfaces are fabricated on silica-based substrates which are highly solvent resistant and electrically insulating using silicate precursor solution (commonly known as “liquid glass”) and concomitant mild heat treatment. We demonstrate the capabilities of such ultraflat gold surfaces by imaging nanoscale objects on top and fabricating microelectrodes as an example application. Because of the simplicity and versatility of the fabrication process, lgTS will have wide-ranging application in imaging, catalysis, electrochemistry, and surface science.



Metallic surfaces with near atomic roughness are increasingly essential to a plethora of applications in surface and interface sciences. These surfaces have found many applications in biology, electrochemistry, and electronics.<sup>1,2</sup> Such surfaces used in conjunction with scanning probe microscopies can facilitate imaging of biomolecules, such as lipids and proteins, and organic and inorganic colloids, such as quantum dots. Gold is an highly inert metal with a high oxidation potential and therefore the material of choice in many electrochemical applications. Crystalline surfaces enable mechanistic studies at interfaces using electrochemistry and other surface science techniques. Gold is also easily and robustly functionalized with thiol ( $-\text{SH}$ )-terminated molecules. Such self-assembled monolayers (SAMs) of thiols on gold are one of the prevalent tools in nanoscience where ultraflat surfaces are extremely valuable.

Furthermore, gold is an important material at visible wavelengths in the increasingly popular field of plasmonics.<sup>3</sup> Plasmonics has a wide range of applications including surface-enhanced Raman scattering (SERS), where surface roughness plays a key role in the million or more-fold signal enhancements commonly observed.

Ultraflat gold substrates have found use in confirming the effect of roughness<sup>4</sup> and to quantify enhancement factors. In short, a simple, low-cost route to ultraflat gold which is compatible with commonly used solvents is enormously valuable to a large range of disciplines.

Traditionally, deposition methods such as sputtering and evaporation are used to obtain metal surfaces. These, however, result in island formation leading to rough surface finishes. A solution has been found by combining these techniques with cleaved single crystals which reveal atomically flat planes. Metal deposition is carried out directly on top, producing near-atomically flat gold surfaces at the interface. After deposition and further processing to add a backing layer to the deposited metal, the crystalline template is removed, revealing the ultraflat gold surface. This is known as template stripped gold (TSG).

A variety of TSG methods have been developed to add a backing layer to the ultraflat metal. Hegner et al.<sup>5</sup> use a mica film

as the template and epoxy glue to attach the gold to a silicon wafer superstrate. While providing a simple and robust method of TSG formation, the weakness of this method is the use of epoxy glue which is sensitive to organic solvents, in which swelling causes distortion of the gold surface. This system also suffers from trapped air bubbles and outgassing, which are problems under vacuum.<sup>6</sup> The epoxy method has been improved by introducing ceramic glues, which are not as severely plagued by organic solvent problems.<sup>7</sup> These epoxies, however, are still not entirely solvent resistant.<sup>6</sup>

A novel epoxy-free approach involves nickel superstrates formed by electroplating onto the conductive gold surface. Nickel is conductive and not completely inert limiting the application of such prepared surfaces in electronics. Gold often prematurely delaminates from the mica surface during nickel electroplating.<sup>8</sup> Most recently, solid-state bonding techniques have been developed which rely on gold diffusion.<sup>2,6,8</sup> Two surfaces, a substrate (gold on mica) and a superstrate (gold on glass), are bonded under pressure and/or heat. Gold ions diffuse between the two metal interfaces, fusing them together. As there is no glue, this method is not affected by solvent-induced swelling, but it suffers from several technical drawbacks. Cold-welding<sup>6</sup> is highly sensitive to surface contamination and is generally not reliable over large areas. This is overcome by heating the gold surfaces during bonding<sup>8</sup> which increases ion mobility, requiring temperatures above  $300^\circ\text{C}$  and pressures up to 4000 psi. The increased mobility leads to significant gold reorganization, which can cause delamination. The only solution is to deposit gold at a high temperature, a capability not available in most evaporators. Although centimeter-sized films have been produced using solid-state bonding by distributing the load using aluminum foil,<sup>8</sup> this advance requires significant optimization. Moreover

**Received:** November 2, 2011

**Revised:** November 30, 2011

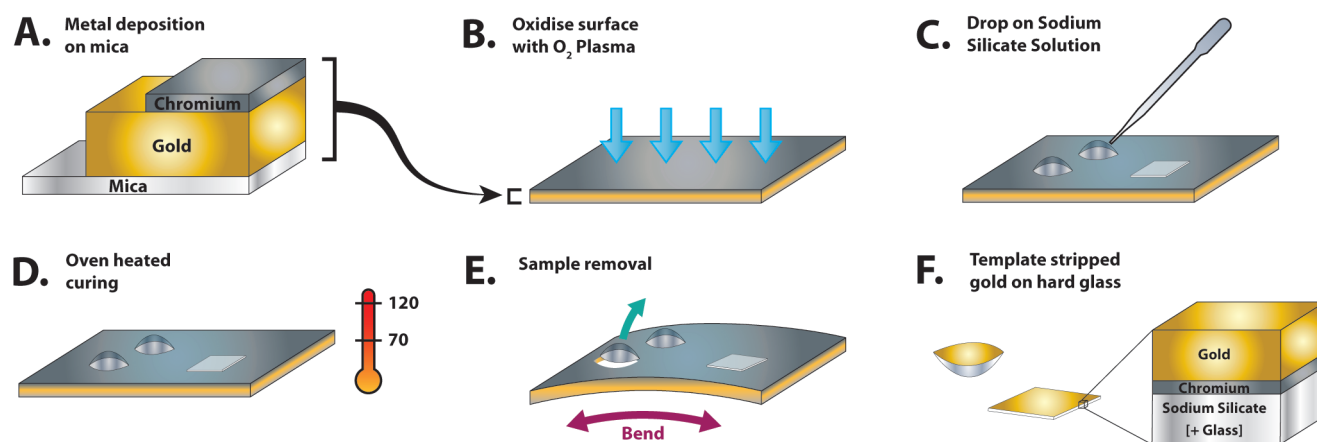


**Figure 1.** IgTSG fabrication schema. (A) Gold (150 nm) and chromium (5 nm) layers are thermally evaporated onto a freshly cleaved mica substrate. (B) Chromium is hydrophilically functionalized by oxygen plasma. (C) Sodium silicate solution (liquid glass) is drop cast onto the chromium surface. Plasma-cleaned glass slides can be placed on top of these droplets to form a sturdier backing. (D) Heating in a two-stage process balances water evaporation and transformation to silica. (E) IgTSG can easily be removed by gently bending the mica. (F) The process results in ultraflat gold backed onto a glass slide or a thin (300  $\mu\text{m}$ ) silica sheet.

patterned designs, such as electrodes, are not possible with solid-state bonding methods due to the difficulty in alignment of evaporation masks. A final variation on TSG to avoid substrate deformation by solvent swelling has been to use solder as the bonding agent. Conventional solders melt around 200  $^{\circ}\text{C}$ , which damages the thin gold film, so low-melting ( $\text{mp} \sim 70\text{ }^{\circ}\text{C}$ ) solders are used. However, these are highly toxic, limiting the ease of creation.<sup>9</sup>

In this paper we present a novel, silica-based approach for fabricating ultraflat gold, called the liquid glass TS (IgTS) method. This process has several advantages over those described above. (1) It is solvent resistant and (2) consists of very few simple steps which are highly reproducible. (3) It is compatible with glass substrates, providing an insulating base. (4) It is able to create large-area ( $>1\text{ cm}^2$ ) substrates as well as (5) patterns with 100  $\mu\text{m}$  sized features. (6) Many samples can be made in parallel, and (7) the process requires only low-cost materials and no specialized evaporation or high-pressure systems. Furthermore, the silica-formed superstrate is transparent at visible wavelengths and is therefore compatible with systems requiring optical access to the back of the gold film. In our process we deposit gold on freshly cleaved mica and then use a liquid silica precursor as both the glue and superstrate. A simple hydrophilic chromium functionalization of the gold surface, and gentle heating, allows this precursor to bond, and harden, respectively. The resulting ultraflat gold is easy to remove from its mica substrate. These procedures are not highly time-sensitive or intensive and do not require a clean-room atmosphere.

## MATERIALS AND METHODS

High grade ruby muscovite 20  $\text{cm}^2$  mica sheets (Agar Scientific), 99.99% pure gold pellets (Birmingham Metal Co.), chromium-plated tungsten rods (Agar Scientific), and sodium silicate solution (Sigma-Aldrich 338443), also known as liquid glass, were used as received. Evaporation was performed on a BOC Edwards Auto 306 resistance evaporator at  $10^{-6}$  mbar. Oxygen plasma treatment was performed using a Diener Electronic Femto plasma system. The samples were dried in a Binder FP programmable oven at 2  $^{\circ}\text{C}/\text{min}$ .

Cadmium selenide QDs (Nanoco Technologies Ltd./Sigma-Aldrich Lumidots 662461) were used to show the imaging potential of the

IgTSG substrates. The solutions were diluted further with toluene before use. Two varying density quantum dot layers were produced: (1) A small drop of low concentration (5  $\mu\text{g}/\text{mL}$ ) solution was drop-cast onto the IgTSG, giving rise to a low QD density. (2) A higher density but still submonolayer coverage of QDs was created via SAM functionalization and QD adsorption.<sup>10</sup>

AFM was performed using a Veeco Nanoscope IV, with an ultrasharp tapping mode tip (Nanosensors PPP-NCHR).

Thermogravimetric analysis (TGA) was performed on a TA Instruments Q500, from 20 to 200  $^{\circ}\text{C}$  at a rate of 1  $^{\circ}\text{C}/\text{min}$  under air.

Wide-angle X-ray diffraction was carried out using a Bruker D8 diffractometer with a  $\text{K}\alpha$  beam of  $\lambda = 1.5406\text{ \AA}$ . Spectra were taken with angular increments of 0.009  $14^{\circ}$  and a dwell time of 0.5 s.

## FABRICATION

Facile fabrication of solvent-resistant ultraflat gold is outlined in Figure 1. 150 nm of gold was thermally evaporated onto freshly cleaved mica. Under continued vacuum, 5 nm of chromium was deposited on top of the gold surface. The use of chromium as an adhesion layer is common between gold and silica surfaces, and this principle was successfully applied in our inverse geometry. All evaporation was done at a rate of 0.2  $\text{\AA s}^{-1}$ . Evaporation masks were used to pattern electrodes.

The chromium layer was exposed to an oxygen plasma for 5 min to deepen the native oxide layer and thus increase hydrophilicity with average water contact angle decreasing from  $65^{\circ}$  to  $<3^{\circ}$ . This allows the silica solution to wet the surface, which ensures uniform drying, and prevents the trapping of air bubbles during this process which can destroy the sample. The oxidized surface also promotes adhesion of the silica network through Si–O bonding. Two types of samples were created, with and without an additional glass slide backing. In the first case, glass slides (1  $\text{cm}^2$ ) were cleaned and oxidized by oxygen plasma to enhance wetting. The slides were drop-coated with 20  $\mu\text{L}$  of sodium silicate solution and immediately inverted and placed onto the oxidized chromium surface. In the second case, for samples without the backing, the sodium silicate solution was drop-cast directly onto the oxidized chromium surface.

Drying and conversion of liquid sodium silicate to a solid silicate network were then achieved by controlled heating to

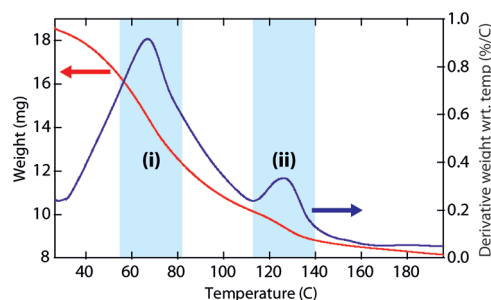


**Figure 2.** Thermogravimetric analysis for sodium metasilicate. Two key regions are identified (i) and (ii), corresponding to water loss from the crystal structure at different temperatures. Heating to higher than 120 °C is necessary to ensure sufficient water is removed from the structure.

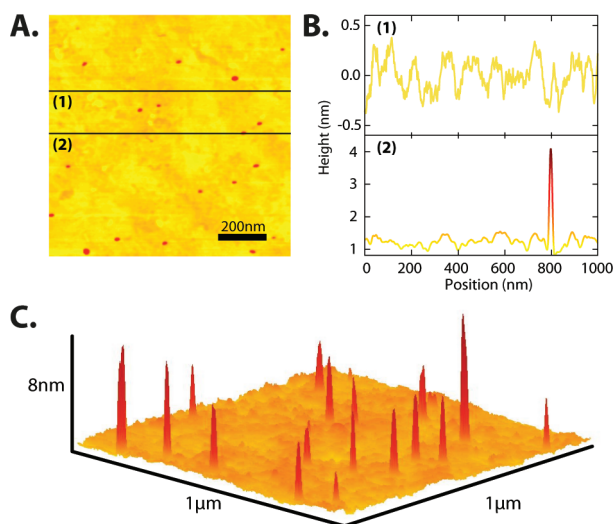


**Figure 3.** (A) AFM image of 6 nm CdSe quantum dots on a flat lgTSG surface. (B) Cross sections showing line height profiles across AFM image of a flat area (1) and over a quantum dot (2). (C) Three-dimensional AFM image of quantum dots on a lgTSG.

ensure bubble-free and low-solubility lgTSG. Samples were heated in a two-stage process, first to 70 °C and then 120 °C, for 12 h each. The lower temperature annealing removes the water from solution but does not provide enough energy to remove water locked into the silicate structure. The higher temperature annealing frees this water, which lowers the hydration state and decreases the solubility of the solid sodium silicate network. The higher the fraction of removed water, the less soluble the silica network.<sup>11–13</sup> Using TGA, we obtained the drying profile shown in Figure 2, showing two distinct drying regions. Region i corresponds to the area where water is fully evaporated from the solution. Further water is released in region ii, corresponding to a change in the silica hydration state. It is necessary to perform the annealing in two stages as direct heating to high temperatures leads to water boiling and the formation of bubbles. The resulting samples can be stored indefinitely in anhydrous conditions. lgTSG samples are easily and quickly removed from the mica substrate when needed by gently flexing the mica sheet.

## DISCUSSION

TSG roughness was characterized using tapping-mode AFM. We repeatably measured an average root-mean-squared (rms)

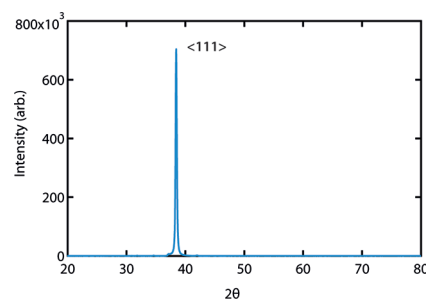


**Figure 4.** 2θ X-ray diffraction spectrum of TSG films showing the dominance of the <111> crystallographic plane.

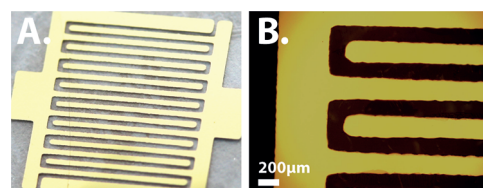


**Figure 5.** (A) Photograph of a 1 cm<sup>2</sup> gold electrode as prepared using the lgTS process. (B) 5× microscope image of the electrode, showing the 200 μm features.

roughness to be 0.275 nm over an area of a square micrometer, confirming the near atomic flatness of the samples. This rms value is equivalent to or better than values quoted in the literature.<sup>5,8,9,14–17</sup>

Because of the ultrasoft nature of lgTSG surfaces, it was possible to clearly image individual QDs, as shown in Figure 3. Ultraflat gold is essential for such measurements because of the small (6 nm) diameter of the QDs. When measured on standard evaporated gold, they are lost in the surface roughness. The employed sample preparation procedure demonstrates one of the advantages of lgTSG, since standard TSG would swell and be destroyed by the deposition of the QDs from toluene.

Oriented crystallinity at the interface is important for catalytic, electrochemical, and surface science studies as surface interactions are dependent on the crystal plane. Hence, X-ray diffraction (XRD) tests were performed to determine the crystallographic properties of the lgTSG thin films. The spectrum in Figure 4 is dominated by the gold <111> reflection peak. Contrary to that from polycrystalline gold, the peaks corresponding to other gold planes are missing.<sup>15</sup> Thus, the lgTSG films consists of <111> coaligned crystals.

Since crystalline surfaces are important in electrochemistry, we demonstrate the ease of patterning using the lgTS process by fabricating micrometer-sized electrodes. An lgTSG interdigitated electrode fabricated using an evaporation mask and the lgTS procedure is shown in Figure 5, illustrating the versatility of the lgTS technique.

Finally, we note that our lgTS technique represents a simple and cost-effective route to fabricate solvent-resistant TSG. Sodium silicate solution is widely available and inexpensive. Competing methods such as those requiring solid-state bonding require specialized equipment and extensive calibration to achieve repeatable samples. The lgTS method is able to repeatably produce reproducible surfaces and many samples in parallel.

## CONCLUSIONS

A simple and inexpensive way of fabricating TSG has been developed, resulting in metal surfaces with 0.275 nm (measured

over  $1\ \mu\text{m}^2$ ) rms surface roughness. The resulting substrate is ultrasmooth, optically transparent, and stable in a wide-variety of organic solvents. The gold is crystallographically aligned in the  $\langle 111 \rangle$  direction. This facilitates easy handling in a chemical environment, often required for working with SAMs, and is therefore advantageous for widespread use in nanoscience. This technique improves over existing methods in terms of sample preparation complexity, cost, and solvent instability, while retaining the same level of surface flatness. Furthermore, we have demonstrated the utility of IgTSG surfaces in imaging nanoscale objects such as quantum dots. We have also shown the ability to pattern ultraflat micrometer-sized structures with the IgTS process which should find widespread use in catalytic, electrochemical, and surface science studies.

## AUTHOR INFORMATION

### Corresponding Author

\*E-mail: jth27@cam.ac.uk (J.T.H.); sm735@cam.ac.uk (S.M.).

### Author Contributions

<sup>†</sup>These authors contributed equally to this work.

## ACKNOWLEDGMENT

We gratefully acknowledge the EPSRC for funding and grants EP/G060649/1 and EP/H028757/1. J.T.H. acknowledges Renishaw Diagnostics Ltd. for funding through an EPSRC CASE studentship. A.S.F. acknowledges the Clerk Maxwell Scholarship for funding.

## REFERENCES

- (1) Love, J.; Estroff, L.; Kriebel, J.; Nuzzo, R.; Whitesides, G. *Chem. Rev.* **2005**, *105*, 1103.
- (2) Blackstock, J.; Li, Z.; Freeman, M.; Stewart, D. *Surf. Sci.* **2003**, *546*, 87.
- (3) Nagpal, P.; Lindquist, N.; Oh, S.; Norris, D. *Science* **2009**, *325*, 594.
- (4) Li, L.; Mahajan, S. Manuscript in preparation.
- (5) Hegner, M.; Wagner, P.; Semenza, G. *Surf. Sci.* **1993**, *291*, 39.
- (6) Blackstock, J.; Li, Z.; Jung, G. *J. Vac. Sci. Technol., A* **2004**, *22*, 602.
- (7) Wagner, P.; Hegner, M.; Guentherodt, H.; Semenza, G. *Langmuir* **1995**, *11*, 3867.
- (8) Mosley, D.; Chow, B.; Jacobson, J. *Langmuir* **2006**, *22*, 2437.
- (9) Weiss, E. A.; Kaufman, G. K.; Kriebel, J. K.; Li, Z.; Schalek, R.; Whitesides, G. M. *Langmuir* **2007**, *23*, 9686.
- (10) Hugall, J. T.; Baumberg, J. J.; Mahajan, S. *Appl. Phys. Lett.* **2009**, *95*, 141111.
- (11) Uchino, T.; Sakka, T.; Iwasaki, M. *J. Am. Ceram. Soc.* **1991**, *74*, 306.
- (12) Shelby, J. E.; McVay, G. L. *J. Non-Cryst. Solids* **1976**, *20*, 439.
- (13) Tomozawa, M.; Erwin, C.; Takata, M.; Watson, E. *J. Am. Ceram. Soc.* **1982**, *65*, 182.
- (14) Jung, B.; Frey, W. *Nanotechnology* **2008**, *19*, 145303.
- (15) Chai, L.; Klein, J. *Langmuir* **2007**, *23*, 7777.
- (16) Ederth, T. *Phys. Rev. A* **2000**, *62*, 062104.
- (17) Samori, P.; Diebel, J.; Lowe, H.; Rabe, J. *Langmuir* **1999**, *15*, 2592.